



OPEN FNDC5 affects invasion and migration of oral cancer by inhibiting PI3K/Akt/Snail signaling pathway

Fang Zhao, Dongyang Xu, Xiumei Wang[✉] & Xiaofeng Wang[✉]

This study first investigated how FNDC5 affected the development of oral cancer and revealed the role of FNDC5 in the migration and invasion of oral cancer. The present work evaluated differential FNDC5 expression within oral cancer samples versus matched non-carcinoma samples based on GEO database analysis and immunohistochemistry. We then generated oral cancer cell lines with FNDC5 overexpression and knockdown to determine the role of altered FNDC5 expression in the migration and invasion of oral cancer. PI3K inhibitor was used for investigating the possible mechanism underlying FNDC5 during EMT of oral cancer. Finally, these in-vitro results were validated using the lung metastatic nude mouse model. According to our results, FNDC5 level markedly decreased within oral cancer compared with adjacent samples and FNDC5 overexpression inhibited migration, invasion as well as EMT of oral cancer, while FNDC5 knockdown promoted oral cancer cell EMT. In addition, PI3K inhibitors blocked the induction of oral cancer cells EMT by FNDC5 knockdown. In vivo experiments further demonstrated the above results. This work is the first to illustrate the impact of FNDC5 on inhibiting migration and invasion of oral cancer, and our results suggest that FNDC5 affects EMT of oral cancer via the inhibition of PI3K/Akt/Snail pathway.

Keywords FNDC5, Oral cancer, Epithelial–mesenchymal transition, Invasion and migration, PI3K/Akt/Snail pathway

Oral cancer is a general term for malignant tumors occurring in the oral cavity, most of which belong to squamous epithelial cell carcinoma. In clinical practice, it may also include salivary adenocarcinoma and other tumors occurring in the glands of the oral cavity^{1,2}. The main factors that promote oral cancer are smoking, alcohol, spicy foods, poor oral hygiene, and human papillomavirus (HPV) infection³. As is the case for other malignant tumors, oral cancer is prone to metastasis and invasion, most commonly to the cervical lymph nodes and lungs, followed by bone, liver, and mediastinal lymph nodes¹, resulting in a poor disease prognosis and high recurrence and mortality rates⁴. Oral cancer treatment, therefore, remains a significant challenge.

Epithelial–mesenchymal transition (EMT) has been extensively identified as a critical mechanism underlying the aggressive nature and metastatic ability of cancers⁵. As a result, tumor cells will acquire mesenchymal properties, accompanied by tumor immune escape, stem cell property maintenance, and drug resistance. The main EMT transcriptional regulators include Zinc-finger E-box-binding homeobox 1 (ZEB1), ZEB2, TWIST, SNAIL, and SLUG⁶. The mechanisms of EMT regulation in cancer have received widespread attention, and EMT has been increasingly suggested to have a critical effect on oral cancer progression⁷. Therefore, therapy targeting EMT is considered a novel therapeutic modality for oral cancer.

Fibronectin type III domain-containing protein 5 (FNDC5), the protein present within cells from various tissues, is recently suggested to have an essential effect on tumor development⁸. Studies have shown significantly increased FNDC5 expression within gastrointestinal cancer samples⁹. Moreover, Liu et al. documented that FNDC5 promoted the proliferation of hepatocellular carcinoma (HCC) cells via PPAR γ /NF- κ B/NLRP3 pathway¹⁰. However, FNDC5 has also been reported to inhibit lung cancer cell growth and invasion via PI3K/AKT pathway¹¹. Additionally, in studies related to osteosarcoma, FNDC5 has been shown to inhibit tumor invasion and migration via STAT3/Snail pathway¹². However, changes in the expression and distribution of FNDC5 in oral cancer have not been explored, and the mechanism it plays in the progression of oral cancer has not been revealed.

Department of Stomatology, The Second Affiliated Hospital of Harbin Medical University, Harbin, China. ✉email: hrbwangmei@163.com; 13633617656@163.com

The present work provided an initial indication of FNDC5's effect on oral cancer development, and by exploring signaling pathways by which FNDC5 affects migration and invasion of oral cancer cells, FNDC5 might affect oral cancer cell EMT via PI3K/Akt/Snail pathway.

Materials and methods

Ethics approval

Pathological tissue sectioning and immunohistochemistry staining experiments involved in this study were performed with assistance from the Department of Pathology, Second Affiliated Hospital of Harbin Medical University, and strictly followed the requirements of the Hospital's Research Ethics Committee. All experiments in the text were carried out in accordance with the relevant guidelines and regulations and under the supervision and guidance of the Medical Ethics Committee of the Second Affiliated Hospital of Harbin Medical University (Ethics Approval No.KY2016-021).

Differences in FNDC5 expression in oral cancer versus non-carcinoma samples based on GEO database

Two OSCC microarrays (i.e., GSE37991 and GSE31056) were downloaded from the GEO database (<https://www.ncbi.nlm.nih.gov/geo/>). The GSE37991 microarray dataset contained 40 OSCC tissues and 40 adjacent non-tumorigenic epithelial tissues. This work adopted the GPL6883 platform file as the gene annotation reference. GSE31056 microarray dataset included 23 OSCC tissues, 49 histologically normal marginal tissues, and 24 adjacent normal tissues, with the GPL10526 platform file being the gene annotation reference. The present study utilized mean probe expression value to match gene expression with several probes. Expression patterns from both datasets could be directly analyzed. A comparison between two groups was conducted using the Wilcoxon rank-sum test, while that was done among three groups using the Kruskal–Wallis test.

Immunohistochemistry

4.0% paraformaldehyde (PFA) was added to fix cancer tissues from 45 oral cancer patients as well as adjacent tissue specimens (The tumor tissues were all oral squamous cell carcinomas, and the paracancerous tissues were those within 2 cm of the tumor tissues), followed by paraffin-embedding and slicing to 4- μ m sections. We used the vacuum negative pressure antigen repair method: ① Slices were dewaxed to water. ② 0.3% H₂O₂ methanol vacuum negative pressure treatment for 5 min. ③ Wash with tap water and distilled water. ④ 0.01 M citrate buffer (PH6.0), vacuum-negative pressure drying oven pre-adjusted to 95 °C, vacuum-negative pressure treatment for 10 min. ⑤ To be restored, injection reduced to room temperature of one, PBS wash 3 times. Afterward, 3.0% hydrogen peroxide together with 5.0% bovine serum was added in sequence to treat sections, followed by overnight FNDC5 antibody (1:200, ab181884, Abcam, Cambridge, MA, USA) and Ki67 antibody (1:3000, 27309-1-AP, Proteintech, China) incubation under 4 °C, another 1-h incubation using a species-specific secondary antibody conjugated with horseradish peroxidase (HRP) under ambient temperature, as well as diaminobenzidine (DAB) and hematoxylin counter-staining. Finally, images of the stained tissues were obtained with the AxioVision Rel 4.6 Computerized Image Analysis System (Carl Zeiss). Later, the tissue staining area and the intensity (area \times intensity) were adopted for assessing the staining degree. Staining area scores were 0–4, which indicated staining area of 0%, 0–10%, 10–35%, 35–75%, and 76–100% separately. On the other hand, staining intensity scores ranged from 0 to 4, indicating non, weak, medium, and strong staining separately. Protein levels were expressed as SI calculated by staining area score \times staining intensity score, and $SI \geq 8$ and < 8 indicated high and low expression separately.

Cell lines and culture

We acquired the human oral cancer cells (Tca8113 and ACC-M) in Shanghai Cell Bank, Chinese Academy of Sciences (Shanghai, China) and cultivated them within the Roswell Park Memorial Institute-1640 (RPMI-1640, HyClone, USA) medium that contained 1% penicillin-streptomycin (HyClone) along with 10% fetal bovine serum (FBS, Excellbio, USA) before later analysis under 37 °C with 5% CO₂.

FNDC5 up-regulation and down-regulation

GeneChem (Shanghai, China) was responsible for constructing the cDNA sequence of human FNDC5, which was later combined with the lentiviral plasmid vector before transfected into cells. Cells overexpressing FNDC5 and negative controls are called OE-FNDC5 and NC1, respectively. siRNAs targeting the FNDC5 gene were provided by RiboBio (Guangzhou, China). The siRNA sequences were (1) GGAUACGGAGUACAUAGUC, (2) GGAUGAGGUUGUCAUCGGA, (3) GAAGAUGGCCUCCAAGAAC. Based on the knockdown effect, Gene Chem constructed a lentiviral plasmid vector targeting FNDC5 using the first sequence and a plasmid containing the hU6-MCS-CMV-Puromycin element sequence. The cells with FNDC5 knockdown and negative controls are referred to as KD-FNDC5 and NC2, respectively.

After that, this work incubated Tca8113 or ACC-M cells (10⁵/well) into the six-well plates for a 12-h period, after which virus solution (10 mL) with 40 mL of infection-enhancing solution was added for transfection. At 24-h later, medium change was completed, followed by an additional 24-h cell culture with 1 μ g/mL puromycin. After transfection, we harvested cells for later analysis.

Cell viability assay

This work cultured oral cancer cells into the 96-well plates by adding 5 \times 10³ cells to all wells, which were later divided into the OE-FNDC5, the KD-FNDC5, and the normal control group, and six duplicate wells were set in every group. Following a 12-h culture, the medium was replaced, and then the Cell Counting Kit-8 (CCK-8) reagent was introduced in line with specific protocols to incubate cells for another 1-h period incubation in an

incubator protected from light. Finally, the microplate reader (BioTek, VT, USA) was adopted for measuring absorbance (OD) values at 450 nm.

Transwell invasion assay

Cell invasion assays were completed using a 24-well Transwell chamber. After coating Matrigel (50 μ L) into the top chamber, this work inoculated 5×10^4 oral cancer cells into serum-free medium (100 μ L) before addition into the top chamber. Later, 600 μ L medium that contained 10% FBS was added into the bottom chamber. After 24 h of incubation, one clean cotton swab was adopted to remove oral cancer cells onto the upper membrane surface. After that, methanol was added to fix cells on the lower membrane surface, followed by crystal violet staining. After selecting nine random areas, the inverted microscope was utilized to count invading cell numbers.

Immunofluorescence staining

E-cadherin serves as the specific marker for EMT. E-cadherin level in oral cancer cells was detected by immunofluorescence staining. After washing with PBS, 4% PFA was supplemented to fix the cells for 1-h. Normal goat serum (Beyotime, Shanghai, China) was added to incubate cells for another 1-h period under 4 °C, and finally, an E-cadherin antibody (1:1000, #3195, Cell Signaling Technology, USA) was added. Afterward, FITC-labeled sheep anti-rabbit IgG (H&L) was added to incubate cells for 2 h at 37 °C in the dark and finally observed and imaged using a fluorescence microscope.

Western-blot (WB) analysis

RIPA buffer was added to the lysis of oral cancer cells at 4 °C to extract the total protein. The total protein fractions were then subjected to SDS/PAGE (10%) for separation and then transferred onto PVDF membranes (Millipore, Bedford, MA, USA). Later, 5% skim milk was added to soak membranes for a 2-h period under room temperature, followed by overnight primary antibody (1:1000, Cell Signaling Technology) incubation under 4 °C. The primary antibodies below were used: N-cadherin (#13116), E-cadherin (#3195), Vimentin (#5741), Snail (#3879), PI3K (#4249), p-PI3K (#17366), Akt (#4691), p-Akt (#4060), FNDC5 (1:2000, ab174833, Abcam, USA), and β -actin (1:5000, #4967, Cell Signaling Technology). The appropriate HRP-coupled secondary antibody was added for 2-h membrane incubation under ambient temperature. Finally, ECL detection reagents (Millipore) were added to incubate membranes, and ImageJ software was employed for protein band intensity analysis. Final results were acquired from three independent replicate experiments.

In vivo metastasis assay

The experimental design protocol using animals gained approval from the Medical Ethics Committee of the Second Affiliated Hospital of Harbin Medical University. All animal experimental studies were conducted in accordance with the ARRIVE guidelines.

We obtained female BALB/c nude mice from Beijing Vital River Laboratory Animal Technology Co., Ltd (Beijing, China), and the lung metastasis model was constructed using ACC-M cells. In brief, each mouse was placed in the 12-h light/dark cycle environment, maintained at 25 ± 1 °C with 56% humidity. Adequate food and water were provided. Fifteen mice 8 weeks of age and with an initial weight between 20 and 23 g were selected for the experiment. An incision of approximately 1 cm was made on the skin surface of the neck to expose the internal jugular vein, followed by injection of 1×10^6 ACC-M cells (0.1 mL) in the vein and skin closure. Based on the difference in the FNDC5 expression in the injected cells, the mice were classified into three groups, containing control ($n=5$), FNDC5 overexpression ($n=5$), and FNDC5 knockdown ($n=5$) groups. On day 42, mice were euthanized by CO₂ inhalation followed by thoracotomy, and the lung tissue was removed and weighed. Specimens were immersed in a 10% formalin solution, and metastases on the lung surface were calculated. At the same time, the mice's lung tissues were sectioned and stained with HE, and the percentage of tumor tissue in each group of sections was counted. Then, the lung metastases were sectioned, and immunohistochemical staining was performed to compare the expression levels of Snail in each group.

Data analysis

The experimental results were examined using GraphPad 7 software (GraphPad Software Inc., CA, USA). Results were represented by means \pm the SEM from three or more separate assays. Differences between the two groups were compared by t-test, while those among several groups were by one-way ANOVA. $P < 0.05$ represented statistical significance.

Results

FNDC5 levels in oral cancers

As revealed by immunohistochemical staining, FNDC5 levels significantly decreased within 40 oral cancer cases compared with surrounding non-carcinoma samples, with no significant difference in FNDC5 expression compared with adjacent tissues in only five oral cancer cases (Fig. 1a, Table 1). According to GEO database analysis, FNDC5 expression remarkably decreased relative to non-carcinoma adjacent tissues (OSCC vs. normal oral tissues: GSE37991, $p=0.0004$; GSE31056, $p=0.0002$.) (Fig. 1b). We then generated oral cancer cells showing FNDC5 up-regulation and down-regulation (KD-FNDC5 vs. control: Tca8113, $p=0.0213$; ACC-M, $p=0.0101$. OE-FNDC5 vs. control: Tca8113, $p=0.0069$; ACC-M, $p=0.0024$.) (Fig. 1c), and through CCK-8 assay, we found that FNDC5 knockdown enhanced oral cancer cell growth, while FNDC5 overexpression suppressed their proliferation (CCK-8 assay, KD-FNDC5 vs. control (48 h): Tca8113, $p=0.0034$; ACC-M, $p=0.0001$. OE-FNDC5 vs. control (48 h): Tca8113, $p=0.0013$; ACC-M, $p=0.0003$.) (Fig. 1d).

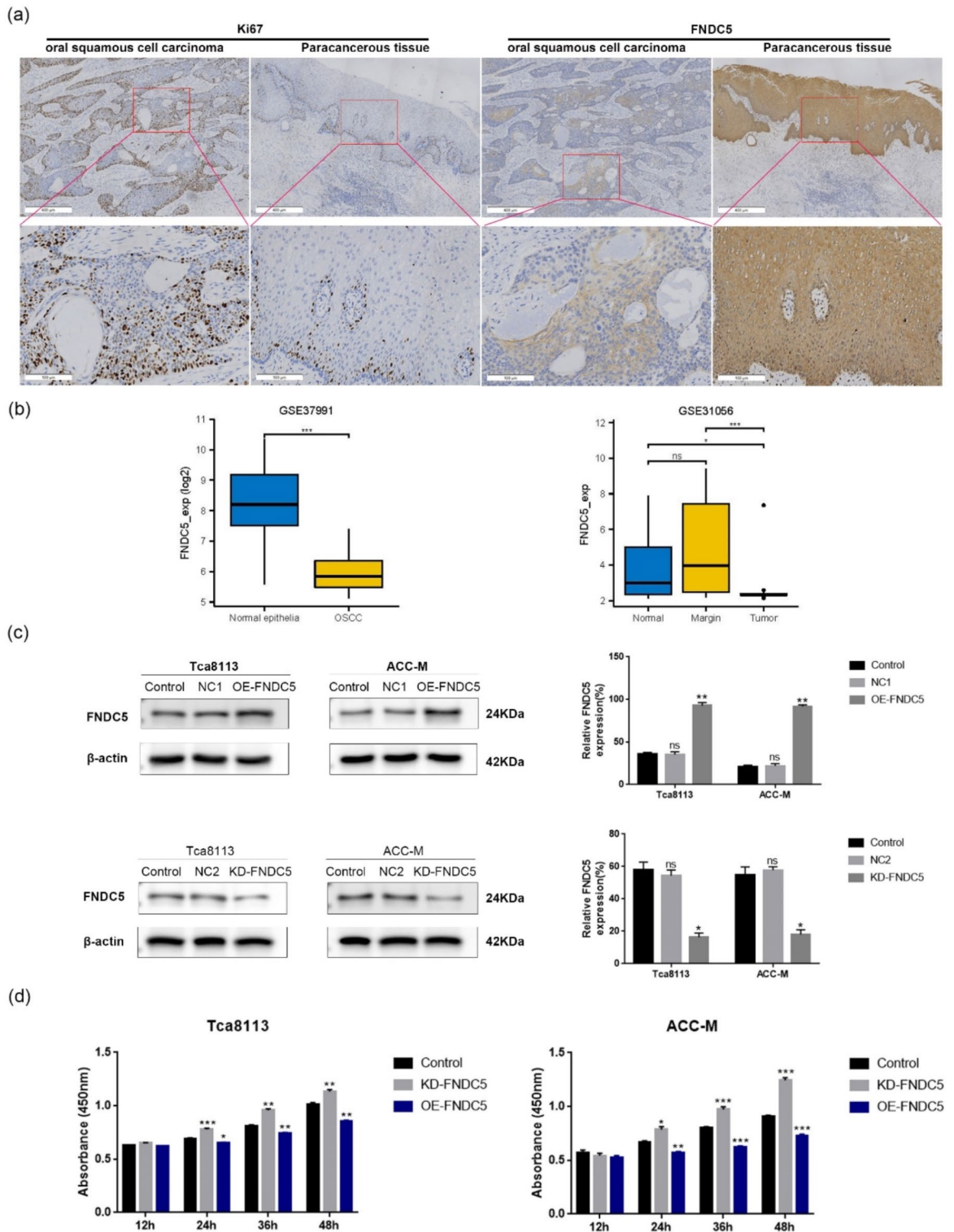


Fig. 1. Lower levels of FNDC5 expression in oral cancer tissues than that in the normal adjacent tissues. (a) Lower level of FNDC5 expression in oral cancer tissues. (b) GEO database analysis showed that the level of FNDC5 expression was lower in oral cancer tissues than that in adjacent tissues. (c) FNDC5 knockdown or overexpression in oral cancer cells using a lentiviral plasmid vector, and the knockdown or overexpression effect was verified by Western blot assay. (d) Effect of FNDC5 knockdown and overexpression on oral cancer cell proliferation measured by CCK-8 assay. *Compared with control, * $p < 0.05$, ** $p < 0.01$, *** $p < 0.001$. ns means no significant difference.

	Total	Expression level (SI)		Positive rate (%)	<i>p</i>
		Low (SI < 8)	High (SI ≥ 8)		
Cancer tissue	40	35	5	87.5	1.01862E-13
Non-cancerous tissue	40	5	35	12.5	

Table 1. Data analysis of immunohistochemistry results.

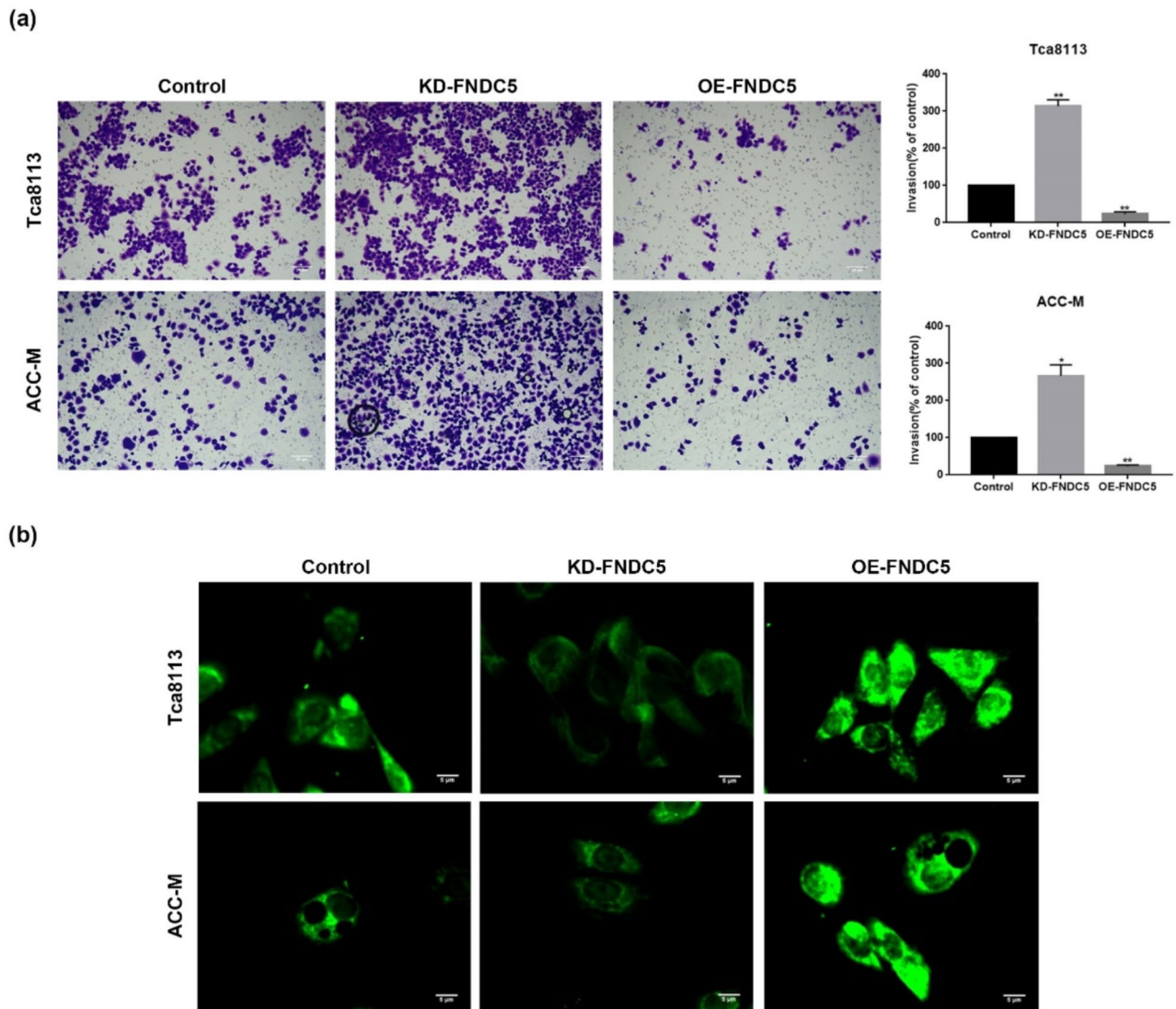


Fig. 2. Effect of changes in the level of FNDC5 expression on oral cancer cell invasion and migration (a) Effect of FNDC5 levels on oral cancer cell invasion and migration determined by Transwell assay. (b) The invasion and migration abilities of three groups of oral cancer cells, Control, KD-FNDC5, and OE-FNDC5, were assessed by E-cadherin immunofluorescence staining. *Compared with control, * $p < 0.05$, ** $p < 0.01$.

FNDC5 inhibits migrations and invasion of oral cancer cells

For analyzing FNDC5's role in oral cancer cell migration and invasion, this work performed Transwell assays for assessing the invasion and migration ability of the OE-FNDC5, the KD-FNDC5, and the normal oral cancer cell lines. As a result, OE-FNDC5 cells had decreased invasion relative to normal oral cancer cell line, while the KD-FNDC5 cell line had an enhanced invasive ability compared with that of the normal oral cancer cell line (Transwell assay, KD-FNDC5 vs. control: Tca8113, $p = 0.0068$; ACC-M, $p = 0.0302$. OE-FNDC5 vs. control: Tca8113, $p = 0.0045$; ACC-M, $p = 0.0017$) (Fig. 2a). In addition, E-cadherin immunohistochemical staining also demonstrated that E-cadherin was up-regulated within OE-FNDC5 cells but was down-regulated within KD-FNDC5 cells (Fig. 2b).

FNDC5 inhibits oral cancer cell EMT

We found that FNDC5 knockdown promoted lung metastasis of oral cancer cells *in vivo*, while FNDC5 overexpression inhibited the formation of lung metastases by oral cancer cells (lung metastatic foci, KD-FNDC5 vs. control: $p=0.0279$; OE-FNDC5 vs. control: $p=0.0306$. Lungs/Body weight, KD-FNDC5 vs. control: $p=0.0117$; OE-FNDC5 vs. control: $p=0.0128$. Metastatic area, KD-FNDC5 vs. control: $p=0.0031$; OE-FNDC5 vs. control: $p=0.0002$.) (Fig. 3a,b). Next, we analyzed the expression levels of Snail protein in lung metastatic tumor sections from each group of mice using immunohistochemistry and found that Snail levels were increased in the group with overexpression of FNDC5 and decreased in the group with knockdown of FNDC5 (Fig. 3c). We then analyzed EMT marker expression, containing E-cadherin, N-cadherin, and Vimentin, within OE-FNDC5, the KD-FNDC5, and the normal oral cancer cell lines by Western blot assay. As a result, E-cadherin (an epithelial cell marker) was up-regulated in the OE FNDC5 oral cancer cell line relative to normal oral cancer cells. In contrast, N-cadherin and Vimentin (the mesenchymal cell markers) expression decreased, thus resulting in inhibition of EMT within these cells. By contrast, the KD-FNDC5 cell line exhibited decreased E-cadherin expression whereas increased Vimentin and N-cadherin levels, thereby facilitating EMT within these cells (KD-FNDC5 vs. control: Tca8113, N-cadherin, $p=0.0179$; Vimentin, $p=0.0155$; E-cadherin, $p=0.0071$. ACC-M, N-cadherin, $p=0.0036$; Vimentin, $p=0.0070$; E-cadherin, $p=0.0023$. OE-FNDC5 vs. control: Tca8113, N-cadherin, $p=0.0077$; Vimentin, $p=0.0073$; E-cadherin, $p=0.0313$. ACC-M, N-cadherin, $p=0.0301$; Vimentin, $p=0.0055$; E-cadherin, $p=0.0211$.) (Fig. 3d).

FNDC5 overexpression inhibits PI3K/Akt/Snail pathway activation

We analyzed the FNDC5-related mechanism by Western blot assays. First, the KD-FNDC5 cell line was treated using LY294002 (a PI3K inhibitor); later, activation levels of the PI3K/Akt/Snail pathway were compared against those of the KD-FNDC5 cell line and the control group and the EMT marker levels were also compared in each group. Our results indicate a high level of PI3K/Akt pathway activation in the KD-FNDC5 cell line (KD-FNDC5 vs. control: Tca8113, p-PI3K, $p=0.0089$; p-Akt, $p=0.0161$. ACC-M, p-PI3K, $p=0.0025$; p-Akt, $p=0.0028$.). N-cadherin and Vimentin expression was decreased, whereas E-cadherin expression increased within KD-FNDC5 cells after exposure to LY294002. Moreover, PI3K/Akt pathway activation by FNDC5 knockdown was reversed, and Snail (a transcription factor, TF) also had decreased expression (KD-FNDC5 + LY294002 vs. KD-FNDC5: Tca8113, N-cadherin, $p=0.0014$; Vimentin, $p=0.0083$; E-cadherin, $p=0.0151$; Snail, $p=0.0093$; p-PI3K, $p=0.0049$; p-Akt, $p=0.0006$. ACC-M, N-cadherin, $p=0.0133$; Vimentin, $p=0.0040$; E-cadherin, $p=0.0302$; Snail, $p=0.0064$; p-PI3K, $p=0.0062$; p-Akt, $p=0.0074$). This suggests that FNDC5's role in the EMT of oral cancer may be associated with the PI3K/Akt/Snail pathway (Fig. 4a). Furthermore, through Transwell and immunofluorescence staining assays, LY294002 was found to suppress KD-FNDC5 oral cancer cell invasion (Transwell assay, KD-FNDC5 + LY294002 vs. KD-FNDC5: Tca8113, $p=0.0092$; ACC-M, $p=0.0132$) (Fig. 4b). Finally, the activation of the PI3K/Akt/Snail pathway in the OE-FNDC5 oral cancer cell line was analyzed. As a result, FNDC5 overexpression inhibited PI3K/Akt/Snail pathway (KD-FNDC5 + LY294002 vs. KD-FNDC5: Tca8113, p-PI3K, $p=0.0269$; p-Akt, $p=0.0054$; Snail, $p=0.0037$. ACC-M, p-PI3K, $p=0.0377$; p-Akt, $p=0.0101$; Snail, $p=0.0033$) (Fig. 4c).

Discussion

FNDC5 is a widely distributed cytokine related to energy metabolism, and initial studies showed that FNDC5 is mainly related to white adipose tissue transformation to brown adipose tissue, mitochondrial oxidation, and energy metabolism^{13,14}. Recently, FNDC5 has served as an antioxidant during cardiomyopathies and kidney diseases^{15,16}, and it alleviates the inflammatory responses induced by illnesses like diabetes or non-alcoholic fatty liver disease (NAFLD)¹⁷. The above studies suggest that FNDC5 seems to affect inflammation as well as oxidation levels in the extracellular environment. Since tumor progression is related to the tumor microenvironment, inflammatory factors, and changes in oxidation levels affect tumor progression, the research on FNDC5 in tumors is gradually increasing¹⁸. Recent studies have shown that in non-small cell lung cancer and liver cancer, FNDC5 expression levels are high and that FNDC5 promotes tumor progression^{19,20}, while in studies related to pancreatic cancer and osteosarcoma, FNDC5 appears to have a tumor-suppressive role^{12,21}. Therefore, the role played by FNDC5 in tumor progression is uncertain and may be caused by the effects of different tumor microenvironments and differences between experimental conditions in individual laboratories²⁰. However, by comprehensively analyzing the currently published articles related to FNDC5, Vliora et al. found that in most cancers, loss of muscle mass leads to reduced levels of FNDC5 in the circulation or in the affected tissues, which makes FNDC5 seem to be able to diagnose cancers independently of other biomarkers, making it a promising independent prognostic factor²². Moreover, so far, the effect of FNDC5 on oral cancer has not been investigated, so it is necessary to explore the effect of FNDC5 in the progression of oral cancer. By analyzing the information from the GEO database, FNDC5 expression was low in oral cancers. Subsequent immunohistochemistry experiments also demonstrated that FNDC5 levels are relatively low in oral cancer tissues. To investigate this further, we generated oral cancer cell lines with FNDC5 knockdown and overexpression. According to preliminary findings based on the CCK-8 assay, FNDC5 overexpression can suppress oral cancer cell growth.

Oral cancer is a common tumor subtype, with approximately 300,000 newly diagnosed cases and 140,000 oral cancer-related deaths each year²³. Due to the susceptibility to metastasis, oral cancer patients are associated with a low (50%) survival rate at 5 years. Therefore, inhibition of oral cancer invasion and metastasis has gradually become an important strategy to improve the prognosis of oral cancer cases²⁴. EMT represents the process where the normal epithelium is gradually transformed into a metastasis-prone mesenchymal phenotype during tumor progression²⁵. In EMT, the epithelial marker E-cadherin is down-regulated, its function diminishes, and intercellular adhesion gradually decreases, while N-cadherin and Vimentin (two mesenchymal cell markers) have increased expression, which causes tumor cells to be shed from their original location^{26,27}, ultimately

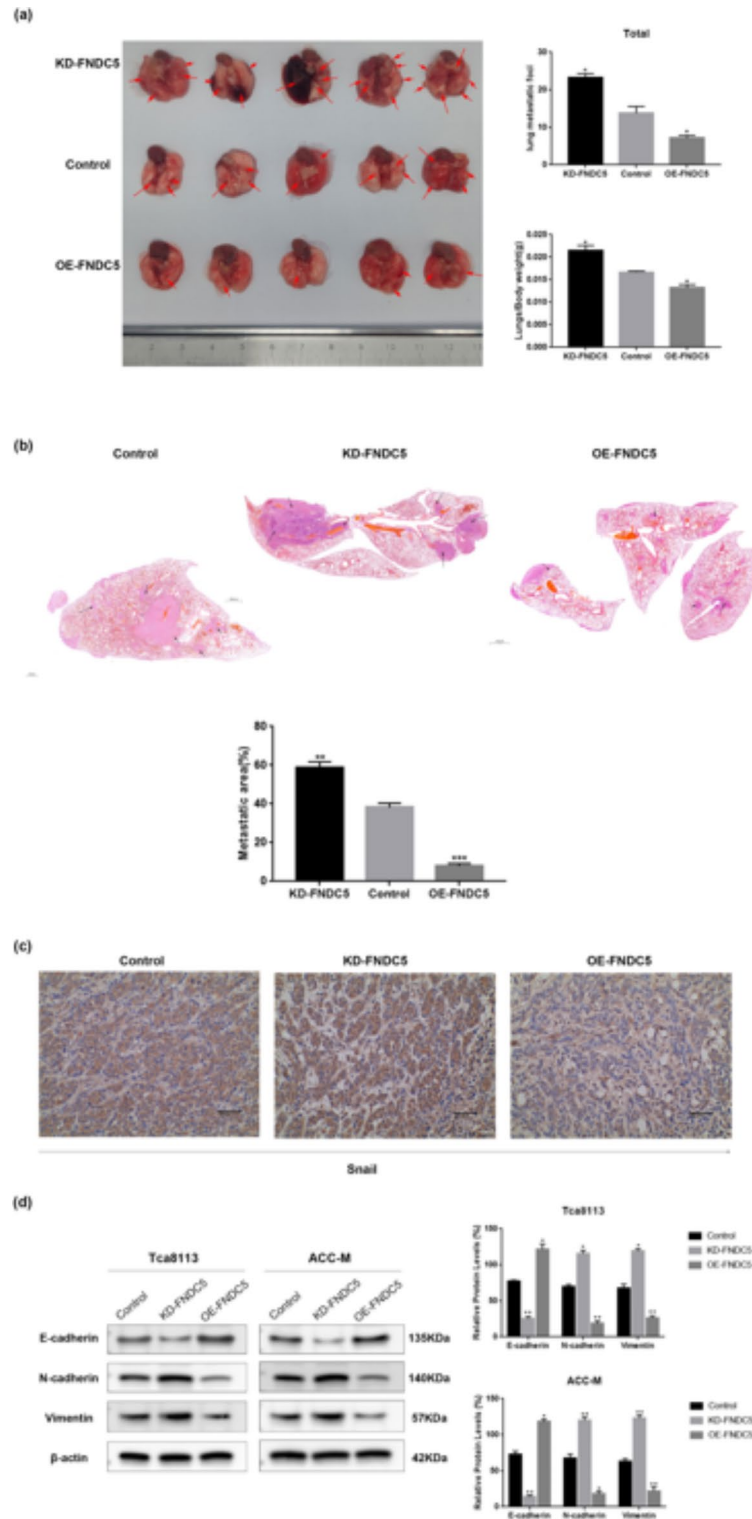


Fig. 3. FNDC5 inhibits oral cancer cell EMT. **(a)** The number of lung metastases formed in vivo by Control, KD-FNDC5, and OE-FNDC5 oral cancer cells, as well as the ratios of the lung-to-body weight. **(b)** HE-stained sections of mouse lung tissues were analyzed and the percentage of metastatic tumor tissue in each group was counted. **(c)** Immunohistochemical methods were used to analyze the level of Snail in lung metastatic tumor sections of mice in each group. **(d)** Effect of FNDC5 on oral cancer cell EMT by Western blot assay. *Compared with control, * $p < 0.05$, ** $p < 0.01$.

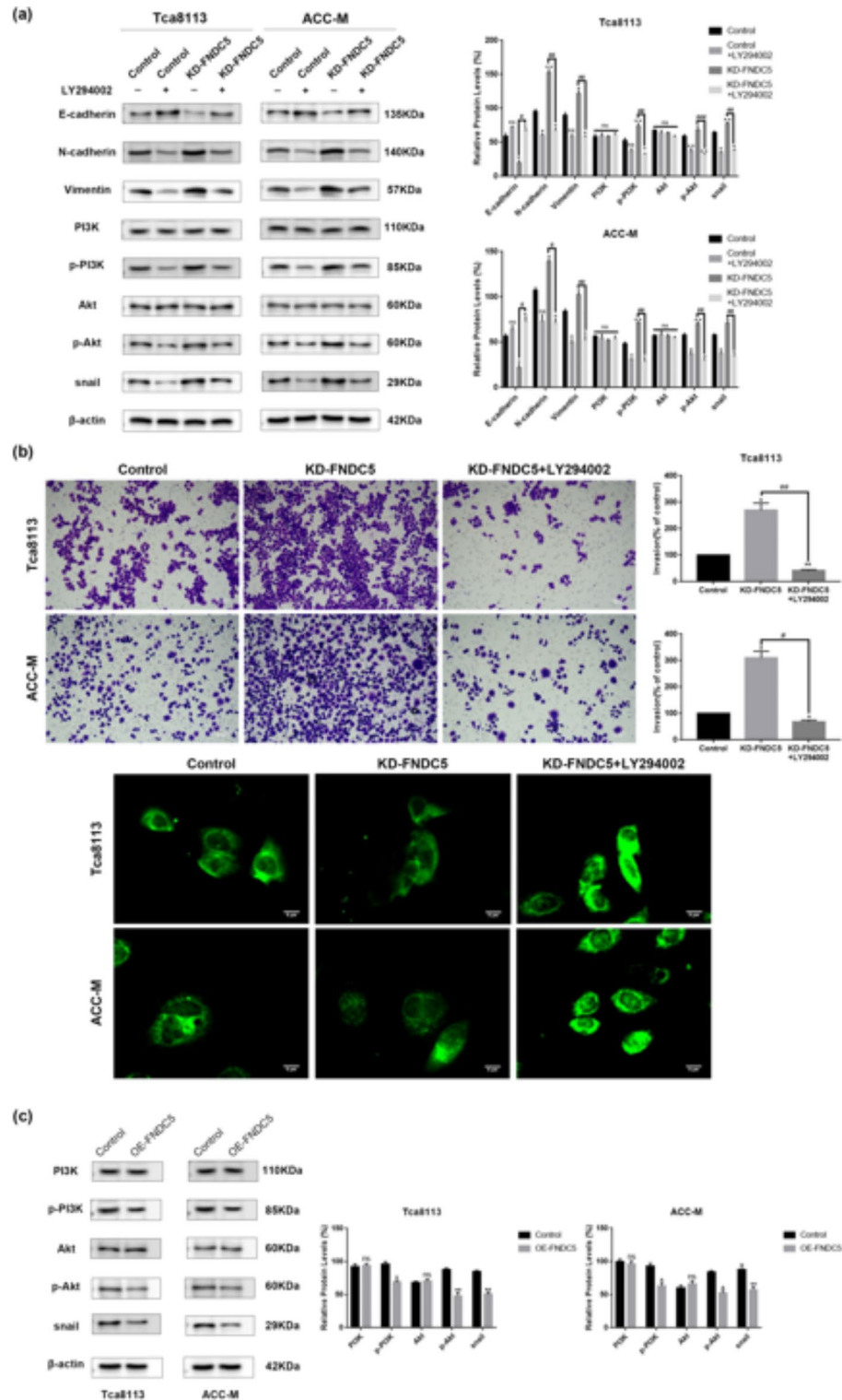


Fig. 4. FNC5 inhibits oral cancer EMT via the PI3K/Akt/Snail pathway. After treatment with LY294002 (5 μM) for 1 h, control and KD-FNDC5 cells were cultured in complete medium for 12 h. **(a)** Western blot assay to detect the expression levels of EMT markers and PI3K/Akt/Snail pathway proteins in each group of cells. **(b)** Transwell and immunofluorescence staining to assess the invasion and migration ability of each group of cells. **(c)** Western blot assay to detect the level of PI3K/Akt/Snail pathway activation in control oral cancer cells and OE-FNDC5 cells. *Compared with control, * $p < 0.05$, ** $p < 0.01$. #Compared with KD-FNDC5 + LY294002, # $p < 0.05$, ## $p < 0.01$, ### $p < 0.001$. ns means no significant difference.

promoting tumor cell metastasis. EMT accounts for the main cause leading to oral cancer development, which is usually regulated by multiple TFs (like Twist and Snail) and signaling pathways²⁸. In previous studies, FNDC5 was shown to inhibit IL-6-induced EMT in osteosarcoma¹²; besides, FNDC5's role in tumor cell migration and invasion has also been reported in ovarian and pancreatic cancers^{21,29}. Based on our Transwell assays and immunofluorescence staining, FNDC5 overexpression suppressed oral cancer cell invasion and migration, while FNDC5 knockdown increased oral cancer cell invasion. According to the results from WB assays, E-cadherin expression elevated, while Vimentin and N-cadherin expression declined within the oral cancer cell line overexpressing FNDC5. In contrast, FNDC5 knockdown resulted in E-cadherin down-regulation, whereas N-cadherin and Vimentin up-regulation in comparison with healthy cells. In related animal experiments, we demonstrated that FNDC5 overexpression inhibited oral cancer cell metastasis.

EMT is previously suggested to be regulated by many signaling pathways, including the TGF- β /Smads, PI3K/Akt, and NF- κ B signaling pathways^{30,31}, with PI3K/Akt pathway promoting EMT mostly by inhibiting Snail phosphorylation, and it increases the stability of Snail protein³². Studies of gastric cancer and lung cancer have demonstrated that PI3K/Akt/Snail pathway activation promotes tumor cell metastasis^{33,34}. Moreover, it has been shown that FNDC5 can affect the proliferation and migration of pancreatic cancer and ovarian tumor cells by inhibiting PI3K/Akt pathway^{21,29}. Alterations of PI3K/Akt pathway activation within FNDC5 overexpression and knockdown cells were analyzed based on previous studies. As a result, FNDC5 overexpression inhibited PI3K/Akt pathway activation and decreased the expression level of Snail proteins compared with normal oral cancer cells. In contrast, FNDC5 knockdown promoted PI3K/Akt/Snail pathway activation, thus promoting EMT. This effect could be reversed by treatment with PI3K inhibitors. Therefore, FNDC5 may inhibit oral cancer EMT by affecting the activation of the PI3K/Akt/Snail pathway.

Conclusions

We first analyzed how FNDC5 affected the migration and invasion of oral cancer cells. According to the obtained findings, FNDC5 suppressed EMT of oral cancer. Our results also indicate that FNDC5 may affect oral cancer cell migration and invasion by inhibiting the PI3K/Akt/Snail pathway. Thus, this work further refines investigation regarding FNDC5's effect on cancers and shows that FNDC5 is closely related to oral cancer invasion and metastasis; developing small molecule agonists targeting FNDC5 may be helpful for inhibiting the metastasis of oral cancer.

Data availability

Two OSCC microarrays (i.e., GSE37991 and GSE31056) were downloaded from the GEO database and are available at the following URL: <https://www.ncbi.nlm.nih.gov/geo/query/acc.cgi?acc=GSE37991>, and <https://www.ncbi.nlm.nih.gov/geo/query/acc.cgi?acc=GSE31056>.

Received: 19 June 2024; Accepted: 30 October 2024

Published online: 06 November 2024

References

- Weisse, J. et al. RNA-Binding proteins as regulators of migration, invasion and metastasis in oral squamous cell carcinoma. *Int. J. Mol. Sci.* **21** <https://doi.org/10.3390/ijms21186835> (2020).
- Montero, P. H. & Patel, S. G. Cancer of the oral cavity. *Surg. Oncol. Clin. N. Am.* **24**, 491–508. <https://doi.org/10.1016/j.soc.2015.03.006> (2015).
- Kumar, K. V. & Hema, K. N. Extracellular matrix in invasion and metastasis of oral squamous cell carcinoma. *J. Oral Maxillofac. Pathol.* **23**, 10–16. https://doi.org/10.4103/jomfp.JOMFP_97_19 (2019).
- Siriwardena, S., Tsunematsu, T., Qi, G., Ishimaru, N. & Kudo, Y. Invasion-related factors as potential diagnostic and therapeutic targets in oral squamous cell Carcinoma-A review. *Int. J. Mol. Sci.* **19** <https://doi.org/10.3390/ijms19051462> (2018).
- Zhang, Y. & Weinberg, R. A. Epithelial-to-mesenchymal transition in cancer: complexity and opportunities. *Front. Med.* **12**, 361–373. <https://doi.org/10.1007/s11684-018-0656-6> (2018).
- Moyret-Lalle, C. et al. Role of EMT in the DNA damage response, double-strand break repair pathway choice and its implications in cancer treatment. *Cancer Sci.* **113**, 2214–2223. <https://doi.org/10.1111/cas.15389> (2022).
- Jayanthi, P., Varun, B. R. & Selvaraj, J. Epithelial-mesenchymal transition in oral squamous cell carcinoma: an insight into molecular mechanisms and clinical implications. *J. Oral Maxillofac. Pathol.* **24**, 189. https://doi.org/10.4103/jomfp.JOMFP_334_19 (2020).
- Cebulski, K. et al. Expression of Irisin/FNDC5 in breast cancer. *Int. J. Mol. Sci.* **23** <https://doi.org/10.3390/ijms23073530> (2022).
- Aydin, S. et al. Irisin immunohistochemistry in gastrointestinal system cancers. *Biotech. Histochem.* **91**, 242–250. <https://doi.org/10.3109/10520295.2015.1136988> (2016).
- Liu, H. et al. FNDC5 induces M2 macrophage polarization and promotes hepatocellular carcinoma cell growth by affecting the PPARgamma/NF-kappaB/NLRP3 pathway. *Biochem. Biophys. Res. Commun.* **582**, 77–85. <https://doi.org/10.1016/j.bbrc.2021.10.041> (2021).
- Shao, L. et al. Irisin suppresses the migration, proliferation, and invasion of lung cancer cells via inhibition of epithelial-to-mesenchymal transition. *Biochem. Biophys. Res. Commun.* **485**, 598–605. <https://doi.org/10.1016/j.bbrc.2016.12.084> (2017).
- Kong, G. et al. Irisin reverses the IL-6 induced epithelial-mesenchymal transition in osteosarcoma cell migration and invasion through the STAT3/Snail signaling pathway. *Oncol. Rep.* **38**, 2647–2656. <https://doi.org/10.3892/or.2017.5973> (2017).
- Liu, J. Irisin as an exercise-stimulated hormone binding crosstalk between organs. *Eur. Rev. Med. Pharmacol. Sci.* **19**, 316–321 (2015).
- Aydin, S. et al. A comprehensive immunohistochemical examination of the distribution of the fat-burning protein irisin in biological tissues. *Peptides.* **61**, 130–136. <https://doi.org/10.1016/j.peptides.2014.09.014> (2014).
- Zhang, R., Ji, J., Zhou, X. & Li, R. Irisin Pretreatment Protects Kidneys against Acute Kidney Injury Induced by Ischemia/Reperfusion via Upregulating the Expression of Uncoupling Protein 2. *Biomed. Res. Int.* **2020**, 6537371. <https://doi.org/10.1155/2020/6537371> (2020).
- Lin, C. et al. FNDC5/Irisin attenuates diabetic cardiomyopathy in a type 2 diabetes mouse model by activation of integrin alphaV/beta5-AKT signaling and reduction of oxidative/nitrosative stress. *J. Mol. Cell. Cardiol.* **160**, 27–41. <https://doi.org/10.1016/j.yjmc.2021.06.013> (2021).

17. Zhu, W. et al. Exercise-induced irisin decreases inflammation and improves NAFLD by competitive binding with MD2. *Cells*. **10** <https://doi.org/10.3390/cells10123306> (2021).
18. Pinkowska, A., Podhorska-Okolow, M., Dziegiel, P. & Nowinska, K. The role of irisin in cancer disease. *Cells*. **10** <https://doi.org/10.3390/cells10061479> (2021).
19. Nowinska, K. et al. Expression of Irisin/FNDC5 in cancer cells and stromal fibroblasts of non-small cell lung cancer. *Cancers (Basel)*. **11** <https://doi.org/10.3390/cancers11101538> (2019).
20. Shi, G. et al. Irisin stimulates cell proliferation and invasion by targeting the PI3K/AKT pathway in human hepatocellular carcinoma. *Biochem. Biophys. Res. Commun.* **493**, 585–591. <https://doi.org/10.1016/j.bbrc.2017.08.148> (2017).
21. Zhang, D. et al. Irisin functions to inhibit malignant growth of human pancreatic cancer cells via downregulation of the PI3K/AKT signaling pathway. *Onco Targets Ther.* **12**, 7243–7249. <https://doi.org/10.2147/OTT.S214260> (2019).
22. Vliora, M. et al. Implication of Irisin in different types of cancer: a systematic review and meta-analysis. *Int. J. Mol. Sci.* **23** <https://doi.org/10.3390/ijms23179971> (2022).
23. Thomson, P. J. Perspectives on oral squamous cell carcinoma prevention-proliferation, position, progression and prediction. *J. Oral Pathol. Med.* **47**, 803–807. <https://doi.org/10.1111/jop.12733> (2018).
24. Chi, A. C., Day, T. A. & Neville, B. W. Oral cavity and oropharyngeal squamous cell carcinoma—an update. *CA Cancer J. Clin.* **65**, 401–421. <https://doi.org/10.3322/caac.21293> (2015).
25. Brabletz, T., Kalluri, R., Nieto, M. A. & Weinberg, R. A. EMT in cancer. *Nat. Rev. Cancer.* **18**, 128–134. <https://doi.org/10.1038/nr.c.2017.118> (2018).
26. Kalluri, R. EMT: when epithelial cells decide to become mesenchymal-like cells. *J. Clin. Investig.* **119**, 1417–1419. <https://doi.org/10.1172/JCI39675> (2009).
27. Wei, S. C. & Yang, J. Forcing through Tumor Metastasis: the interplay between tissue rigidity and epithelial-mesenchymal transition. *Trends Cell. Biol.* **26**, 111–120. <https://doi.org/10.1016/j.tcb.2015.09.009> (2016).
28. Lamouille, S., Xu, J. & Derynck, R. Molecular mechanisms of epithelial–mesenchymal transition. *Nat. Rev. Mol. Cell. Biol.* **15**, 178–196. <https://doi.org/10.1038/nrm3758> (2014).
29. Zhu, T. et al. Irisin/FNDC5 inhibits the epithelial–mesenchymal transition of epithelial ovarian cancer cells via the PI3K/AKT pathway. *Arch. Gynecol. Obstet.* **306**, 841–850. <https://doi.org/10.1007/s00404-022-06427-1> (2022).
30. Niederst, M. J. & Benes, C. H. EMT twists the road to PI3K. *Cancer Discov.* **4**, 149–151. <https://doi.org/10.1158/2159-8290.CD-13-1030> (2014).
31. Sabbah, M. et al. Molecular signature and therapeutic perspective of the epithelial-to-mesenchymal transitions in epithelial cancers. *Drug Resist. Updat.* **11**, 123–151. <https://doi.org/10.1016/j.drup.2008.07.001> (2008).
32. Zhou, B. P. et al. Dual regulation of snail by GSK-3beta-mediated phosphorylation in control of epithelial–mesenchymal transition. *Nat. Cell. Biol.* **6**, 931–940. <https://doi.org/10.1038/ncb1173> (2004).
33. Liu, L., Ye, Y. & Zhu, X. MMP-9 secreted by tumor associated macrophages promoted gastric cancer metastasis through a PI3K/AKT/Snail pathway. *Biomed. Pharmacother.* **117**, 109096. <https://doi.org/10.1016/j.biopha.2019.109096> (2019).
34. Zhou, F. et al. FAM83A signaling induces epithelial–mesenchymal transition by the PI3K/AKT/Snail pathway in NSCLC. *Aging (Albany NY)*. **11**, 6069–6088. <https://doi.org/10.18632/aging.102163> (2019).

Acknowledgements

Our thanks should go to Editage [www.editage.cn] for editing the English language.

Author contributions

F.Z. wrote the main manuscript text. D.X. prepared Figs. 1, 2, 3 and 4. X.M.W. performed manuscript editing and ethical review. X.F. W. provided funding support. All authors reviewed the manuscript.

Funding

The present study was funded by grants from the National Natural Science Foundation of China (Grant No. 8167110215).

Declarations

Competing interests

The authors declare no competing interests.

Additional information

Supplementary Information The online version contains supplementary material available at <https://doi.org/10.1038/s41598-024-78391-6>.

Correspondence and requests for materials should be addressed to X.W. or X.W.

Reprints and permissions information is available at www.nature.com/reprints.

Publisher's note Springer Nature remains neutral with regard to jurisdictional claims in published maps and institutional affiliations.

Open Access This article is licensed under a Creative Commons Attribution-NonCommercial-NoDerivatives 4.0 International License, which permits any non-commercial use, sharing, distribution and reproduction in any medium or format, as long as you give appropriate credit to the original author(s) and the source, provide a link to the Creative Commons licence, and indicate if you modified the licensed material. You do not have permission under this licence to share adapted material derived from this article or parts of it. The images or other third party material in this article are included in the article's Creative Commons licence, unless indicated otherwise in a credit line to the material. If material is not included in the article's Creative Commons licence and your intended use is not permitted by statutory regulation or exceeds the permitted use, you will need to obtain permission directly from the copyright holder. To view a copy of this licence, visit <http://creativecommons.org/licenses/by-nc-nd/4.0/>.

© The Author(s) 2024